JOURNAL OF MATERIALS SCIENCE: MATERIALS IN MEDICINE 9 (1998) 567–574

Mechanical properties and corrosion resistance of Ti–6Al–7Nb alloy dental castings

E. KOBAYASHI, T. J. WANG, H. DOI, T. YONEYAMA, H. HAMANAKA
Institute for Medical and Dental Engineering, Tokyo Medical and Dental University, Kanda-surugadai, Chiyoda-ku, Tokyo 101, Japan

With the aim of applying a novel titanium alloy, Ti–6Al–7Nb, to a dental casting material, a comprehensive research work was carried out on its characteristics, such as castability, mechanical properties and corrosion resistance in the present study. As a result, Ti–6Al–7Nb alloy exhibited sufficient castability by a dental casting method for titanium alloys and enough mechanical properties for dental application. It is also showed excellent corrosion resistance through an immersion test in 1.0% lactic acid and an anodic polarization test in 0.9% NaCl solution. From these results, it is concluded that this Ti–6Al–7Nb alloy is applicable as a dental material in place of Ti–6Al–4V alloy, which includes cytotoxic vanadium.

1. Introduction

Much attention has been focused on titanium application in medical and dental fields owing to its superior properties, such as relatively low density, high corrosion resistance and satisfactory biocompatibility [1–3]. However, its mechanical strength is not sufficient for some of the applications [4]. Although recent scientific and technological progress has made it practicable to utilize titanium as a dental casting material [4], it is still necessary to improve the mechanical properties by alloying, for wider application in dentistry.

Ti–6Al–4V (Ti–10.2Al–3.6V at %) alloy, which possesses good strength through desirable microstructure, and consists of α and β phases, has been used widely as a high-strength biomedical alloy. But it has been pointed out that vanadium, an alloying element, has relatively strong cytotoxicity [5, 6]. When a metallic material is exposed to the body fluids for a long time, corrosive reaction is inevitable. Because Ti–6Al–4V alloy contains vanadium as an alloying element, which stimulates mucous in the respiratory organs and is harmful to the blood production system [7, 8], it is necessary to develop a new titanium alloy having good biocompatibility as well as sufficient strength.

Because vanadium and niobium belong to the Va group, they show similar common characteristics, especially the effect to stabilize β phase in the Ti–V and the Ti–Nb binary systems, which is necessary to provide $\alpha + \beta$ two-phase structure to the alloys. Hence, niobium was used as a ternary element to produce the desirable microstructure in the Ti–6Al–7Nb (Ti–10.5Al–3.6Nb at %) alloy, in place of vanadium [9]. The cytotoxicity of niobium was reported to be far less, of the order of 1/1000, than that of vanadium in the solutions with fixed atomic percentages of their ions [10, 11]. This Ti–6Al–7Nb alloy has been standardized for orthopaedic application as a wrought material [12].

In order to evaluate the possibility of applying Ti–6Al–7Nb alloy to a dental casting material, comprehensive examinations were carried out on mechanical properties, castability and corrosion resistance.

2. Experimental procedure

2.1. Materials and specimen preparation

Ti–6Al–7Nb alloy (Daido) was used in this study, and grade 3 titanium (Selec) and Ti–6Al–4V alloy (Selec) were used as the reference materials. All of the specimens were prepared by the precise dental casting technique under the manufacturer's instructions using wax models.

In order to evaluate castability as a function of casting condition, two types of mould material, which were silica-based mould (Snow White, Shofu) and magnesia-based mould (Selevest-CB, Selec), and two types of casting machines, were used. Generally, titanium casting machines specialized for dental casting, consist of a melting portion to remelt an ingot in an inert atmosphere, and a casting portion to push the molten metal into a mould. For the latter portion, two different types of force, i.e. a gas pressure and a vacuum suction type and centrifugal force type, were utilized. The former provides less contamination to castings with interstitial gas elements during the melting and casting processes, while the latter shows less casting defects, such as porosity, due to its relatively large force to push the molten metal into the mould cavity. In this study, two types of casting machines, the gas pressure and vacuum suction type (Castmatic T, Iwatani) and the centrifugal force type (Ticast Super-R, Selec) were chosen to vary the casting conditions.

0957–4530

2.2. Tensile test

Tensile testing was conducted to investigate the mechanical properties as well as the castability of the alloys. The specimens used were 3.0 mm diameter, 20.0 mm long at a parallel portion and 6.0 mm diameter at a chucking portion in accordance with ISO [13]. All the specimens were made by a lost wax dental casting method.

To ensure the accuracy of the evaluation of castability, five specimens for each condition were prepared, and all of the specimens were adopted into the tensile test regardless of the defect. The castability of the alloys as a function of the casting condition, i.e. difference in mould materials and casting machines, was evaluated through apparatus observation of castings and the frequency of accidental rupture by casting defects in an early stage of the tensile test.

The tensile test was carried out at room temperature using an Instron-type testing machine (AG-2000B, Shimadzu) with a strain rate of $8.3 \times 10^{-4}\,s^{-1}$ ($1.66 \times 10^{-5}\,ms^{-1}$ in crosshead speed). Data of load and strain were obtained from a load cell and a strain gauge extensometer. All these data were analysed using a personal computer.

2.3. Hardness measurement

In order to evaluate the surface contamination layer after the casting into a magnesia-based mould, hardness measurement on the transverse cross-section of the Ti–6Al–7Nb alloy cast specimen, 3.0 mm diameter, was conducted using a novel type of hardness tester (DUH-200, Shimadzu).

The hardness value, DH, is defined as the ratio of load and surface area of an impression marked by an indentor, as in conventional Vickers hardness [2]. The indentor was controlled electro-magnetically at a fixed loading rate to a designated load, which was kept for a determined load-holding time. The surface area of the impression marked on the surface was calculated geometrically from the indentation depth and the dimensions of the indentor. Because the indentation depth was measured automatically, personal errors in measurement were eliminated from the hardness value obtained by this tester. The testing conditions were: loading rate at $1.41 \times 10^{-2}\,N\,s^{-1}$, fixed load of 0.49 N and load holding time for 10 s. Hardness measurement was carried out from centre of the specimen to the surface at intervals of 100 μm.

2.4. Immersion test

Cast specimens made of Ti–6Al–7Nb alloy, pure titanium and Ti–6Al–4V alloy, having the dimensions of 20 mm × 10 mm × 1 mm, were prepared through the dental casting technique using the centrifugal-type casting machine and magnesia-based moulds. Specimens were polished up to #800 grid emery paper.

The immersion solution was 1.0% lactic acid [14]; 20.0 ml solution and specimens were put into polyethylene vessels. The quantification of released ions was carried out with the use of an inductively coupled plasma emission spectrometer (ICP, PS3000, Leeman Labs), after the immersion test at 310 K. The vessels were continuously shaken horizontally at 1.67 Hz during the immersion test. The immersion solution was renewed after each ICP analysis. The amount of released ions was summed cumulatively in each period of the test. Five specimens were tested for each metal, and the amounts of dissolved component ions per unit surface of the specimen were evaluated.

2.5. Anodic polarization test

Specimens were prepared using the same casting conditions with the same dimensions as those for the immersion test. The testing surface was mirror-polished, then covered with adhesive Teflon tape® punched a 6.0 mm diameter circular hole for the opening of the test surface.

About 500 ml 0.9% NaCl solution was used as an electrolyte for the test. The solution was deaerated by argon bubbling for at least for 1.8 ks prior to the test and the bubbling was maintained during the test. A platinum electrode was used as the counter electrode, and a saturated calomel electrode (SCE) as the reference electrode.

The exposed surface of the specimen was kept immersed in the solution for at least 1.8 ks until the free corrosion potential, E_{corr}, was settled. Potential scanning was carried out at 310 K from the free corrosion potential to the anodic side up at 3.0 V, and then reversed to the cathodic side up to -0.5 V at a sweeping rate of $1.0\,m\,V\,s^{-1}$. Specimens were washed in water immediately after the test.

2.6. Surface observation

Surface observation of the specimens used for the immersion test and the anodic polarization test was carried out by scanning electron microscopy (SEM, JSM-6400, JOEL) under 20 kV acceleration.

3. Results

3.1. Evaluation of castability

The apparatus observation of cast specimens was carried out prior to the tensile test as one of the factors to evaluate castability. The existence of casting defects and surface reaction, such as oxidation, were checked carefully. The results are shown in Table I. Cast specimens with use of the silica-based moulds were covered with a thick dull oxide layer, while specimens made with magnesia-based moulds exhibited a slightly tarnished metallic surface.

Stress–strain curves of the Ti–6Al–7Nb alloy cast under different conditions are shown in Figs 1–3. For each condition, five specimens were subjected to the tensile test whether or not obvious defects existed, and all the results are indicated in the figures. Obviously, four specimens from five ruptured accidentally before showing normal yield behaviour with the use of the silica-based moulds and the gas pressure and vacuum suction-type casting machine, as shown in Fig. 1. Large casting defects, such as porosities 1 or 2 mm in diameter, were commonly observed on the fractured

TABLE I Results of the castability of Ti–6Al–7Nb and Ti–6Al–4V (reference material) alloys as a function of casting conditions, such as mould materials and casting machines

Materials	Types of mould and casting machine	Appearance	Achievement rate of casting	Assessment
Ti–6Al–7Nb	Silica-based mould Pressure and suction	Dull oxide	1/5	×
	Magnesia-based mould Pressure and suction	Metallic surface	3/5	△
	Magnesia-based mould Centrifugal	Metallic surface	5/5	○
Ti–6Al–4V	Silica-based mould Centrifugal	Dull oxide	1/5	×
	Magnesia-based mould Centrifugal	Metallic surface	5/5	○

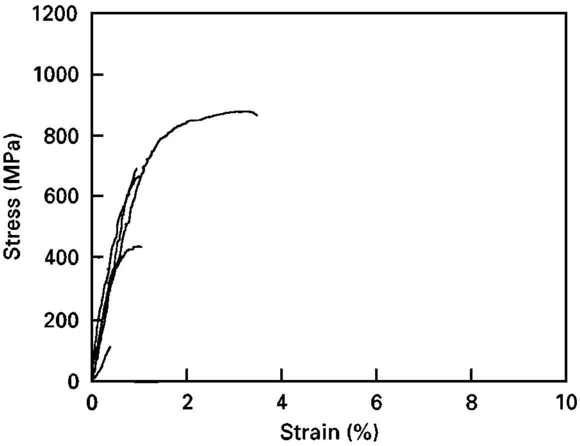

Figure 1 Stress–strain curves of the specimens prepared with silica-based moulds and a gas pressure and vacuum suction-type casting machine. Only one specimen showed normal deformation behaviour.

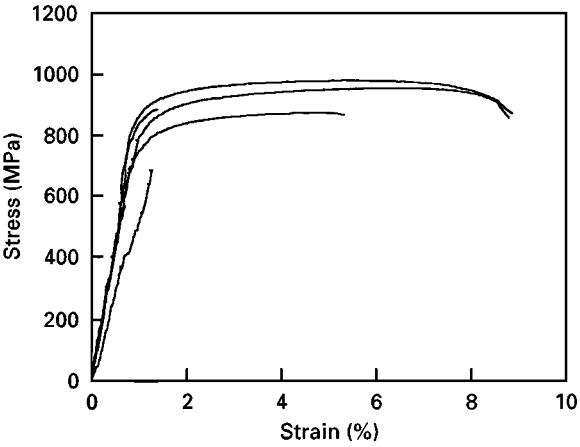

Figure 2 Stress–strain curves of the specimens prepared with magnesia-based moulds and a gas pressure and vacuum suction type casting machine. Three specimens out of five exhibited normal yield behaviour and more than 5% strain.

surface of the specimens ruptured in the early stage of the tensile test. The frequency of good specimens evaluated from these stress–strain curve figures is indicated in Table I as 1/5 in the achievement rate of casting column. This is another factor for judging castability.

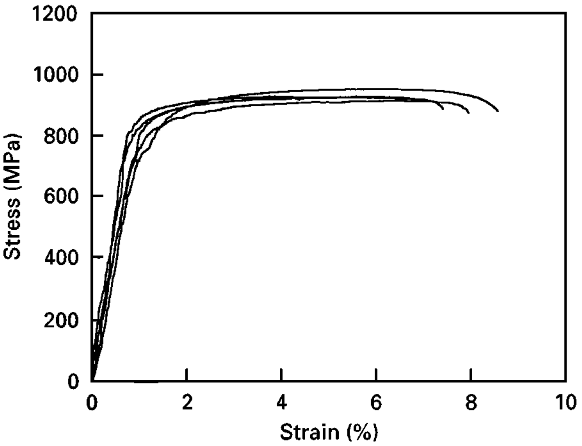

Figure 3 Stress–strain curves of the specimens prepared with magnesia-based moulds and a centrifugal-type casting machine. All five specimens exhibited good tensile test results with a certain strength and approximately 8% total strain.

On substitution of the magnesia-based mould for the silica-based one (Fig. 2), three specimens showed normal yielding and ruptured at more than 5% strain. In contrast, all of the specimens made with magnesia-based moulds and by the centrifugal-type casting machine survived, with normal deformation behaviour until rupture showing around 7% total elongation on average, as shown in Fig. 3.

Overall assessment of castability as a function of casting conditions is indicated in Table I by classification into three levels marked as ×, △ and ○, which indicate poor, moderate and good, respectively, together with the assessment for Ti–6Al–4V alloy, the reference alloy. The best results of castability were obtained under the same conditions for both alloys.

3.2. Tensile test

In the above investigation on the castability of titanium alloys, the best castings were obtained using the magnesia-based moulds and the centrifugal-type casting machine. Mechanical properties of Ti–6Al–7Nb alloy were investigated and compared with those of the reference materials through the tensile test with the specimens prepared under the best casting conditions. The results, i.e. 0.2% proof stress, ultimate

TABLE II Mechanical properties of Ti–6Al–7Nb alloy and reference material evaluated through the tensile test using cast specimens

Materials	0.2% proof stress (MPa)	UTS (MPa)	Total elongation (%)
Ti–6Al–7Nb	816.6 (36.9) [a]	933.2 (14.0)	7.07 (1.62)
Pure titanium	388.4 (12.0)	453.3 (11.0)	23.2 (11.8)
Ti–6Al–4V	883.7 (22.6)	975.5 (42.7)	5.09 (2.17)

[a] Standard deviation is given in parentheses.

tensile stress (UTS) and total elongation, are shown in Table II.

0.2% proof stress and UTS of Ti–6Al–7Nb alloy were slightly less than those of Ti–6Al–4V alloy, while total elongation of the former alloy was much larger than the latter alloy. The strength of grade 3 titanium was approximately half that of titanium alloys.

3.3. Transverse hardness measurement

In order to evaluate the surface contamination layer of the Ti–6Al–7Nb alloy casting, hardness measurement on the transverse cross-section was conducted. Hardness distribution in the cross-section of the specimen cast with the magnesia-based mould by the centrifugal-type casting machine is indicated in Fig. 4.

The hardness of the internal area was around 300 DH, where less contamination from the mould materials could affect the property. The hardness increased to about 420 DH at a point 25–50 μm beneath the surface.

3.4. Immersion test

In the appearance of the specimens after the immersion test, neither obvious evidence of corrosion nor corrosive products were observed. Fig. 5 shows the amount of titanium ions released from the specimens during the immersion test, detected by an ICP spectrometer. The result of the control, which contained only the immersion liquid, was less than the minimum sensitivity of the spectrometry at each period of the test.

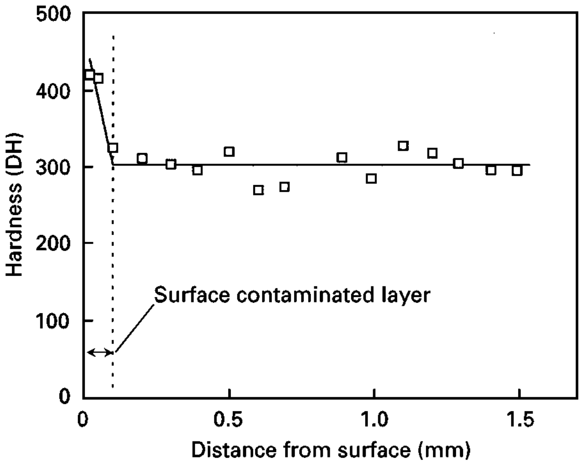

Figure 4 Hardness measurement on the transverse cross-section of the specimen, 3 mm diameter, cast using magnesia-based moulds and a centrifugal-type casting machine, showing around 100 μm thick surface contaminated layer.

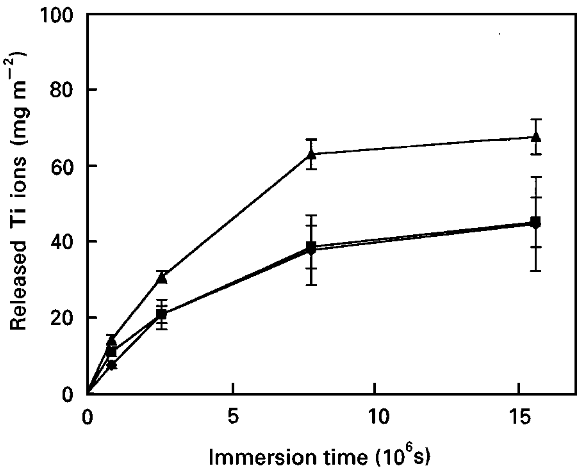

Figure 5 Titanium ions released from the specimens during the immersion test using 1.0% lactic acid at 310 K, detected by ICP spectrometry. (■) Ti–6Al–7Nb, (◆) pure titanium, (▲) Ti–6Al–4V.

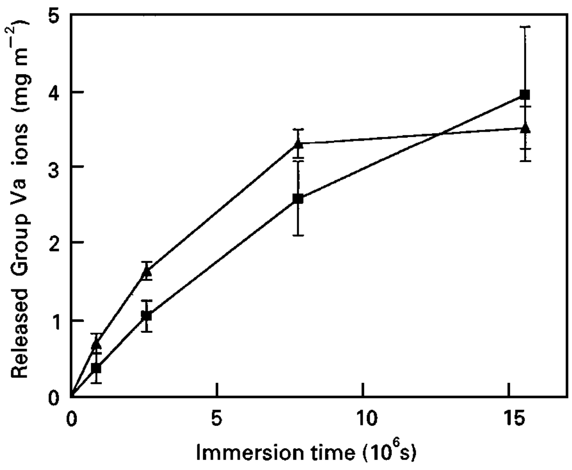

Figure 6 Comparison of Group Va ions released from (■) Ti–6Al–7Nb and (▲) Ti–6Al–4V alloys during the immersion test in 1.0% lactic acid at 310 K.

The amount of titanium ions released from every material increased with increasing immersion time. The relation between the released amount and the immersion time was not proportional, but parabolic. The amount of titanium ions released from Ti–6Al–7Nb alloy was less than from Ti–6Al–4V alloy and comparable to that from titanium. The aluminium ion content in these alloys was not investigated, because of the difficulty in accurately detecting low concentrations of aluminium.

Fig. 6 shows the variation in the amount of niobium and vanadium ions released from Ti–6Al–7Nb and Ti–6Al–4V alloys, respectively. Although the amounts of both Va group ions are comparable in this figure, it is suggested that Ti–6Al–7Nb alloy is less corrosive than Ti–6Al–4V alloy in this 1.0% lactic acid, considering that the atomic weight of niobium is approximately 80% larger than that of vanadium. This is consistent with the difference in titanium ions released from these alloys, as mentioned above.

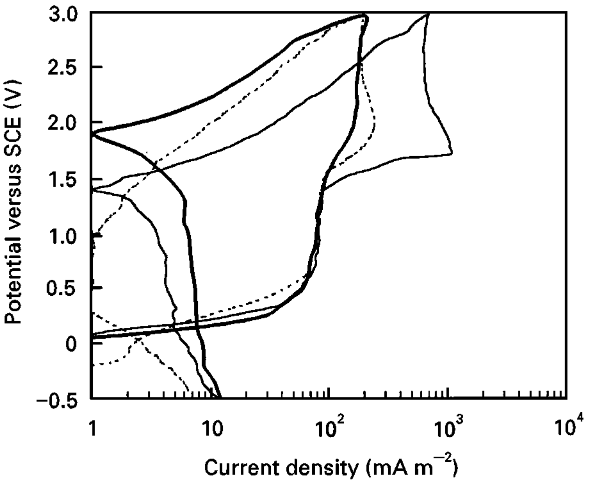

Figure 7 Comparison of anodic polarization curves of (——) Ti–6Al–7Nb alloy and reference materials, ((—) pure titanium and (– – –) Ti–6Al–4V alloy) tested in 0.9% NaCl solution.

3.5. Anodic polarization test

The anodic polarization test is a method of evaluating the corrosion property of a metallic material from the relation between the current density per unit surface area and the potential scanned artificially. The current density directly indicates the dissolution of metallic ions from the material into the electrolyte, namely the state of corrosion.

A typical anodic polarization curve generally consists of an active state, a passive state and a transpassive state. In the active state, the current density increases rapidly with increasing potential; this results in the formation of an oxidized layer on the surface. In the passive state, the increase in current density is reduced and settles at a particular level due to the protective effect of the passive film formed in the previous state. By adding further potential, the passive film starts to be broken and the current density again increases steeply.

To evaluate formability and stability of a passive film, i.e. the corrosion resistance of a material, the free corrosion potential, E_{corr}, critical passivation current density, I_{erit}, passivation holding current density, I_{ps}, and transpassivation potential, E_{tp}, are introduced from an anodic polarization curve. For example, a passive film is evaluated to be formed easily when the critical passivation current density is low, and it is stable if the passivation holding current density is low. It is inferred that the passive film is firm if the transpassivation potential is large, and the corrosion resistance can be evaluated from the current density through the overall potential range.

Typical results of the anodic polarization test are shown in Fig. 7. By applying the potential scanned from the free corrosion potential, E_{corr}, to the anodic side, the current density increased steeply and entered the passive state without showing a peak of the critical passivation current density, I_{crit}, in all samples. The passivation holding current density, I_{ps}, at the passive state, which is around 80–90 mA m^{-2}, continued until approximately 1.5 V of potential versus SCE in each specimen, and was followed by another arresting of the current density at a higher level. In the base-directed scanning of the anodic polarization curve after once reaching 3.0 V potential, the behaviour varied with the materials. Ti–6Al–7Nb alloy exhibited the lowest current density of the three materials. The obvious transpassivation potential, E_{tp}, was not seen in the potential range scanned in this study, which was up to 3.0 V.

3.6. SEM observation of the specimen after the corrosion tests

Fig. 8 shows scanning electron micrographs of the specimen surfaces (a) before and (b) after the immersion test. No conspicuous difference was observed between (a) and (b), and the specimen surfaces still shed metallic lustre after the immersion test for 15.6×10^6 in 1.0% lactic acid.

Because the specimens for the immersion test were finished by polishing with #800 emery papers, scratches can be seen in these micrographs. The edge of the scratch was considered to be easily affected by the corrosion. In spite of careful examination, there was no obvious evidence of dissolution, even at these the edges, which were still sharp in (b).

SEM observation was also carried out on the anodic polarization test specimens which had a mirror-polished surface. No evidence of pitting corrosion was observed in the specimens after the test.

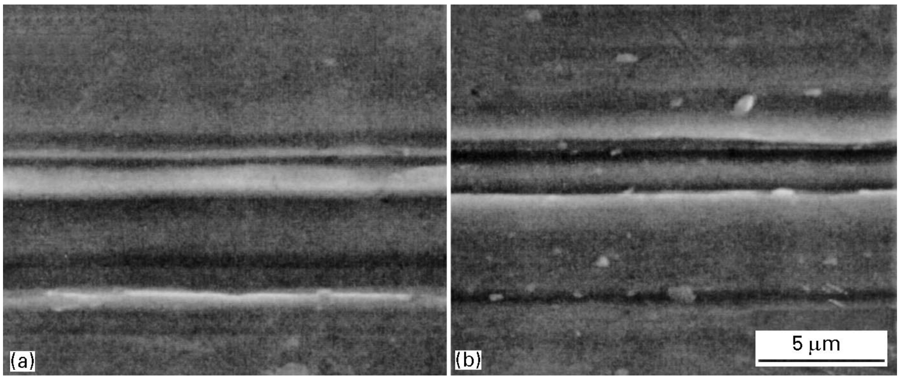

Figure 8 Scanning electron micrographs of the Ti–6Al–7Nb alloy specimen used for the immersion test, (a) before the test, (b) after the test for 15.6×10^6 ms.

4. Discussion

4.1. Castability of Ti–6Al–7Nb alloy and nature of the castings

The casting conditions with the magnesia-based mould and the centrifugal type casting machine exhibited the best castability in the present study, as shown in Table I. The standard free energy of magnesia formation is negative and larger than that of titanium oxide (TiO_2), while that of silica formation is slightly negative, and smaller than that of TiO_2, which means silica is less stable than TiO_2 [15]. Hence, the silica in the mould would be deoxidized by molten titanium in the casting process, resulting in the formation of TiO_2 on the surface of the castings. This oxide was observed on the surface of the specimens cast with the silica-based mould, as indicated in Table I. On the other hand, the specimens made with the magnesia-based mould had no conspicuous oxide on the surface and maintained their metallic colour. Owing to the difference in the standard free energy, titanium is not easily oxidized by the oxygen in magnesia. A slight tarnishing with interference shine was observed on the surface, which is believed to be caused by a thin TiO_2 layer.

The flow of molten metal in the mould cavity is thought to be controlled by some factors, such as viscosity of the molten metal, casting pressure acting on the metal, and the reaction between the metal and the mould materials. The type of casting machine most likely influences the second factor, and the difference in mould material affects the third one, as mentioned above. In the range of experiments conducted in this study, the centrifugal-type casting machine appeared to provide the desirable force to push the molten metal into the cavity.

In the hardness measurement on the transversel cross-section of a cast specimen made with the magnesia based-mould, a hardened surface layer, around 100 μm thick, was observed just beneath the surface. This hardness change is believed to be caused by the contamination of the surface layer by impurity elements during the casting process. It was reported that the hardness and the thickness of the surface layer varied with the mould materials. In the case of pure titanium castings with a silica-based mould material, the surface layer was approximately four times harder than the internal hardness, and the castings made with the magnesia-based mould were about twice as hard, while the thickness was around 100 μm in both cases [16].

In the present study on Ti–6Al–7Nb alloy, the hardness of the surface layer was about 1.4 times harder than the internal hardness, which is smaller than the hardness change of pure titanium in the reference. Because the internal hardness of Ti–6Al–7Nb alloy was larger than pure titanium, due to its refined microstructure consisting of α and β phases, the effect of interstitial elements in the surface layer became relatively smaller than for pure titanium with the α single phase. The thickness of the hardened layer of Ti–6Al–7Nb alloy was almost the same as that of the pure titanium castings.

It is worth mentioning that Ti–6Al–7Nb alloy showed a relatively small standard deviation in total elongation as given in Table II, which may mean less deterioration due to the casting defects.

4.2. Mechanical properties of Ti–6Al–7Nb alloy

To expand the dental application of titanium, it is necessary to improve the mechanical properties. Alloying is one of the effective approaches, and the Ti–6Al–7Nb alloy presented in this paper is thought to be a solution. Niobium, which belongs to group Va in the Periodic Table as does vanadium, works as a β stabilizing element to provide a desirable α+β two-phase structure in place of vanadium in Ti–6Al–4V alloy. With respect to the mechanical properties of Ti–6Al–7Nb alloy castings, as indicated in Table II, the strength of Ti–6Al–7Nb alloy is a few per cent less than that of Ti–6Al–4V alloy, while the ductility of the former is about 40% larger than the latter. The strength of Ti–6Al–7Nb alloy, around 800 MPa in 0.2% proof stress and more than 900 MPa in UTS, were approximately twice that of pure titanium, which was considered to be sufficient for a high-strength dental casting material.

The difference between the strength of pure titanium and Ti–6Al–7Nb alloy is attributed to alloying effects, including solid-solution strengthening and structure-refining strengthening provided by the refined two-phase structure. On the other hand, the difference between the strength of Ti–6Al–7Nb alloy and Ti–6Al–4V alloy can be explained by these two factors. The Goldschmidt atomic radii of niobium and vanadium are 0.147 and 0.136 nm, respectively, while that of titanium is 0.147 nm [17]. Assuming that the solid-solution strengthening results mainly from the size misfit of atoms, the addition of vanadium may provide larger strengthening than niobium due to its larger size misfit.

Secondly, the difference in their microstructure must be considered. Fig. 9 indicates the α + β two-phase field in the Ti–Nb and the Ti–V binary systems [18, 19]. It is clear that the β stabilizing effect of niobium is larger than that of vanadium, because both the α transus and the β transus of the Ti–Nb system

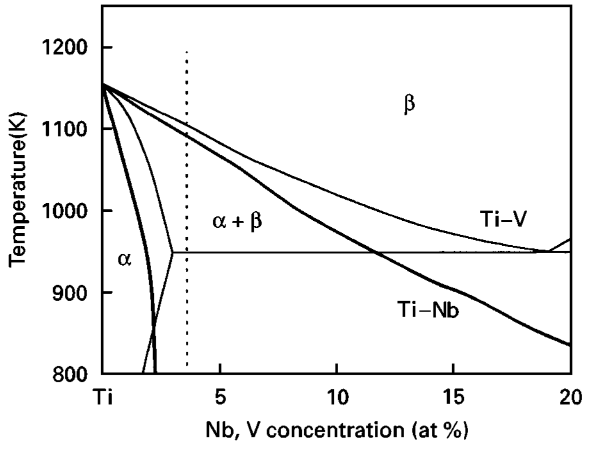

Figure 9 Comparison of the α+β two-phase field in the (——) Ti–Nb and the (—) Ti–V binary systems, after Murray [18].

are shifted toward the α-phase side, as compared with the Ti–V system. This must influence the volume fraction of α and β phases in the two-phase alloys containing the same amount of niobium or vanadium. A vertical broken line indicates 3.6 at% of the alloying elements. According to the phase diagrams of these alloys at 1000 K, the α : β in Ti–3.6 at % Nb alloy is estimated to be around 7 : 3, while that in Ti–3.6 at % V alloy is about 9 : 1. These α : β ratios were estimated for the Ti–Nb and the Ti–V binary systems and did not include the effect of aluminium, an α-phase stabilizer. Nevertheless, the comparison of Ti–6Al–7Nb alloy Ti–6Al–4V alloy may show the same tendency, because both ternary alloys contain the same amount of aluminium. This difference in volume fraction is believed to cause their mechanical properties.

4.3. Corrosion resistance of Ti–6Al–7Nb alloy in the physiological environments

The corrosion resistance is one of the most important characteristics for biomedical materials, because it concerns not only the devices' service life but also their harmfulness in the living body. Thus, it is necessary to evaluate it as a part of a comprehensive research study of a new dental alloy.

As shown in Fig. 4, the corrosion resistance of Ti–6Al–7Nb alloy was found to be better than Ti–6Al–4V alloy and comparable to pure titanium through the immersion test in 1.0% lactic acid. Although 0.9% NaCl solution is widely used as a standard method to evaluate the corrosion resistance of the biomedical materials. 1.0% lactic acid was chosen as an immersion liquid in this study, because it is known to be a more severe corrosive environment than 0.9% NaCl solution. The NaCl solution is believed to be less corrosive from examination of the corrosion resistance of titanium alloys. It is reported that the concentration of titanium ions released from a pure titanium specimen into 0.9% NaCl solution during the immersion test for 15.6×10^6 was less than the minimum sensitivity of the ICP analysis [14].

The anodic polarization test was carried out in order to evaluate the corrosion resistance of the materials precisely. As shown in Fig. 7, the anodic polarization curves indicated the obvious passive state with the passivation holding current density, I_{ps}, at around 80–90 m Am^{-2} without showing a peak in the critical passivation current density, I_{crit}. This absence of a peak is commonly seen in the anodic polarization curves of titanium alloys, especially in the case of testing in a neutral electrolyte, because the passive film on titanium alloys is initiated very rapidly, usually in several seconds. The current density in the passive state was almost the same in each specimen, and the passive state continued up to 1.5 V potential versus SCE, followed by further arrest of the current density at a higher level. Although the reason for this second stage of arrest in the current density has not yet been confirmed, the same phenomenon was observed in a recent study using pure titanium specimens and 1.0% NaCl solution, conducted by other investigators [20].

Although it is difficult to discuss the relation between the results of the anodic polarization test using NaCl solution and that of the immersion test which was carried out in lactic acid, the existence of a protective layer on the sample surface was suggested by both results. The parabolic relation observed in ion concentration during the immersion test suggested the existence of a protective layer and its growth. Further circumstantial evidence was the lack of a peak in the critical passivation current density before the passive state in the anodic polarization test. This protective layer has functioned up to at least approximately 1.5 V potential versus SCE.

An obvious difference was seen in comparison of each curve in base direction scanning after reaching 3.0 V potential versus SCE. This portion of the curves corresponds to the reformation process of the passive film, once broken in the transpassive state. The curve for the Ti–6Al–7Nb alloy lies at the lowest position of current density for the specimens, suggesting a better corrosion resistance in the repassivation in the test.

During SEM observation, no large dissolution was confirmed in the specimens after either the immersion test or the anodic polarization test.

5. Conclusion

With the aim of dental application of a novel titanium alloy, Ti–6Al–7Nb, as a casting material, comprehensive research was carried out on its characteristics, such as castability, mechanical properties and corrosion resistance in the present study.

The best result in the castability was obtained in the case of casting using the magnesia-based moulds and the centrifugal-type casting machine. Specimens had metallic surfaces after casting, without any oxide layer, and showed no accidental rupture due to casting defects during the tensile tests. It was also found that the dental casting techniques developed for casting pure titanium or Ti–6Al–4V alloy, including the mould materials and the casting machines, can be applied to the casting of Ti–6Al–7Nb alloy.

The cast specimens of this alloy exhibited sufficient mechanical properties for use as a base material for dental devices. Its strength was comparable to Ti–6Al–4V alloy which has been used as a high-strength titanium alloy. Additionally, the ductility of Ti–6Al–7Nb alloy was larger than that of Ti–6Al–4V alloy.

Finally, Ti–6Al–7Nb alloy showed superior corrosion resistance to Ti–6Al–4V alloy through the immersion test in 1.0% lactic acid and the *anodic polarization test* in 0.9% NaCl solution. It is comparable to that of pure titanium. It was believed that the Ti–6Al–7Nb alloy maintains sufficient corrosion resistance in the physiological environments for use as dental devices.

From the results obtained through this comprehensive study, it is concluded that this Ti–6Al–7Nb alloy has the potential to be applicable as a dental casting material in place of the conventional materials, such a pure titanium and Ti–6Al–4V alloy, which is still subject to controversy over the alloying element's cytotoxicity.

References

1. H. HAMANAKA and T. YONEYAMA, *Boushoku Gijutsu* **38** (1989) 333.
2. E. KOBAYASHI, S. MATSUMOTO, H. DOI, T. YONEYAMA and H. HAMANAKA, *J. Biomed. Mater. Res.* **29** (1995) 943.
3. H. DOI, M. KOTAKE, T. YONEYAMA and H. HAMANAKA, *Rep. Inst. Med. Dent. Eng., Tokyo Med. Dent. Univ.* **28** (1994) 64.
4. E. KOBAYASHI, H. DOI, M. TAKAHASHI, T. NAKANO, T. YONEYAMA and H. HAMANAKA, *J. Jpn. Soc. Dent. Mater. Devices.* **14** (1995) 406.
5. R. C. BROWNE, *Br. J. Ind. Med.* **12** (1955) 57.
6. F. H. HULCHER, *Spectrophotometric Biol. Mater.* **32** (1960) 1183.
7. S. G. SJOBERG, *Acta Med. Scand.* **154** (1956) 381.
8. S. G. SJOBERG and K -G. RIGNER, *Nord. Hyg. Tidskr.* **37** (1956) 217.
9. M. F. SEMLITSCH, H. WEBER, R. M. STEICHER and R. SCHÖN, *Biomater.* **13** (1992) 781.
10. A. YAMAMOTO, R. HONMA and M. SUMITA, *J. Jpn Soc. Biomater.* **14** (1995) 158.
11. A. YAMAMOTO, T. KOBAYASHI, N. MARUYAMA and M. SUMITA, *ibid.* **14** (1996) 167.
12. ASTM F 1295-92 (American Society for Testing and Materials, Philadelphia, PA, 1992).
13. ISO 6871 (1987).
14. T. YONEYAMA, H. DOI and H. HAMANAKA, *J. Jpn. Soc. Biomater.* **11** (1993) 71.
15. L. S. DARKEN and R. W. GURRY, in "Physical Chemistry of Metals" (McGraw-Hill, New York, 1953) p. 349.
16. H. DOI, T. YONEYAMA, M. KOTAKE and H. HAMANAKA, *J. Jpn Soc. Dent. Mater. Devices* **13** (1992) 817.
17. C. J. SMITHELLS, in "Metals Reference Book", 4th Edn, Vol. 1, (Butterworths, London, 1967) p. 140.
18. J. L. MURRAY, in "Phase Diagrams of Binary Titanium Alloys" (ASM International. Metals Park, OH, 1987) p. 188.
19. *Idem, ibid.*, p. 319.
20. H. MIMURA and Y. MIYAGAWA, *J. Jpn Soc. Dent. Mater. Devices* **15** (1996) 283.

Received 30 July
and accepted 16 September 1997